Journal of Power Sources 194 (2009) 369–380

Contents lists available at ScienceDirect

Journal of Power Sources

journal homepage: www.elsevier.com/locate/jpowsour

A wavelet-fuzzy logic based energy management strategy for a fuel cell/battery/ultra-capacitor hybrid vehicular power system

O. Erdinc, B. Vural, M. Uzunoglu*

Department of Electrical Engineering Yildiz Technical University, Istanbul 34349, Turkey

ARTICLE INFO

Article history:
Received 16 March 2009
Received in revised form 26 April 2009
Accepted 27 April 2009
Available online 3 May 2009

Keywords:
Battery
Fuel cell
Fuzzy logic
Hybrid electric vehicle
Ultra-capacitor
Wavelet transform

ABSTRACT

Due to increasing concerns on environmental pollution and depleting fossil fuels, fuel cell (FC) vehicle technology has received considerable attention as an alternative to the conventional vehicular systems. However, a FC system combined with an energy storage system (ESS) can display a preferable performance for vehicle propulsion. As the additional ESS can fulfill the transient power demand fluctuations, the fuel cell can be downsized to fit the average power demand without facing peak loads. Besides, braking energy can be recovered by the ESS. This study focuses on a vehicular system powered by a fuel cell and equipped with two secondary energy storage devices: battery and ultra-capacitor (UC). However, an advanced energy management strategy is quite necessary to split the power demand of a vehicle in a suitable way for the on-board power sources in order to maximize the performance while promoting the fuel economy and endurance of hybrid system components. In this study, a wavelet and fuzzy logic based energy management strategy is proposed for the developed hybrid vehicular system. Wavelet transform has great capability for analyzing signals consisting of instantaneous changes like a hybrid electric vehicle (HEV) power demand. Besides, fuzzy logic has a quite suitable structure for the control of hybrid systems. The mathematical and electrical models of the hybrid vehicular system are developed in detail and simulated using MATLAB®, Simulink® and SimPowerSystems® environments.

1. Introduction

The considerable increase in global warming and the desire to decrease the dependence on depleting fossil fuels in order to ensure an uninterrupted energy supply have led to much research in alternative energy sources, recently. Specifically, transportation area has a major position in energy consumption and the greenhouse gas emissions causing global warming. Therefore, interest in new solutions for the replacement of conventional internal combustion engine (ICE) based propulsion systems in vehicular applications has increased steadily. Among alternative powertrains, fuel cell (FC) technologies have been proposed as a potential and attractive solution for vehicular applications due to providing environment friendly operation with the usage of renewable fuel [1]. Particularly, the Proton Exchange Membrane FC (PEMFC) emerges as one of the most promising candidates for electric vehicle systems thanks to its simplicity, viability, quick start up, higher power density, relatively high electrical efficiency compared to an approximately sized ICE, and operation at lower temperatures [2].

However, the unsteady operation of a vehicle may not be appropriate for the usage of a sole FC system. The power demand of a vehicle motor undergoes significant variations due to acceleration, changes in road surface and traffic conditions. Thus, a sole FC system may not totally satisfy the power demand of a vehicle by the reason of the limitation of fuel cells to track fast load variations due to their slow response dynamics. Besides, load demand fluctuations in vehicle operation may cause fuel starvation, flooding, membrane drying, and pressure imbalance across the FC membrane, which will damage the FC stack and decreases its lifetime [3]. Moreover, if the FC system alone supplies all power demand, it would increase the size and cost of the FC system as well as hydrogen consumption. Lastly, commercially available fuel cells are not reversible and they do not have capability to recycle the braking energy. Therefore, hybridizing FC system with an energy storage system (ESS) decreases system cost, improves dynamic performance of overall vehicle system, promotes FC lifetime and provides fuel economy owing to regenerative braking energy capturing.

In many hybrid applications, batteries are utilized as ESS [4]. Among the various existing rechargeable batteries, lithium-ion batteries appear to occupy a prime position in various aspects [5]. However, in spite of providing a significantly high energy density potential, commercially available battery systems present some drawbacks, such as low cycle-life, long recharging time and

* Corresponding author. Tel.: +90 212 383 2447; fax: +90 212 259 4869.
E-mail addresses: uzunoglu@yildiz.edu.tr, mehmet_uzunoglu@yahoo.com (M. Uzunoglu).

0378-7753/$ – see front matter © 2009 Elsevier B.V. All rights reserved.
doi:10.1016/j.jpowsour.2009.04.072

low power densities. Besides, rapidly changing current values may damage the chemical structure of batteries. Thus, the usage of a battery system alone as ESS in an automotive powertrain may not be efficient adequately. As an alternative to the battery systems, ultra-capacitors (UCs) – also known as super-capacitors or double-layer capacitors – have drawn attention for use as ESS [6]. UCs present considerably higher power densities than that of batteries, and extremely higher energy densities than that of conventional electrolytic capacitors. The capability for delivering high power/current values in a significantly short time without facing a structural damage is a key advantage over available battery technologies. However, the energy densities of UCs are significantly lower than battery systems [7]. Thus, a battery/ultra-capacitor hybrid ESS for vehicular applications can combine the merits of high energy density of lithium-ion batteries with the high power density of ultra-capacitors to completely meet the vehicle requirements [8].

Owing to the fact that FC, battery and UC have different features and dynamic characteristics, an overall energy management strategy should be designed for the system to coordinate the power flows among the different energy sources. First of all, the power demand of a HEV should be shared between the available on-board power sources considering their individual dynamics. To develop such a load sharing algorithm for FC, battery and UC hybrid structure, we employed wavelet transform owing to its great capability for analyzing and capturing the transients in an applied signal like HEV power demand [9,10]. Thus, the negative effects of instantaneous changes on the electrochemical structures of FC and battery can be prevented. Despite the fact that the wavelet transform may perform an effective performance as a load sharing algorithm, providing an energy management system based only on wavelet transform may not be sufficient enough for regulating all the system power flow. Considering the SOC values of battery and UC, FC system output power should be decreased when both sources have enough charge. Besides, FC system should supply more power if both ESSs have a low SOC level. Thus, the overall system power flow should be controlled in order to increase fuel economy and promote system performance. Thus, a control strategy must be implemented for the developed energy management strategy, so as to guarantee the hybrid system prosperity. For the control of the hybrid system, fuzzy logic controller (FLC) is utilized considering the fact that FLC has a quite suitable structure for the control of hybrid energy systems as used in many studies [4,8,11]. Besides, in order to model the power demand of a HEV and test the performance of the developed energy management algorithm, urban dynamometer driving schedule (UDDS) data is used. Using this dynamic load profile, the hybrid system performance can be evaluated effectively.

In this paper, an energy management system composed of a wavelet-fuzzy logic based load sharing and control algorithm is implemented for the dynamic PEMFC/Battery/UC hybrid vehicular power system model. This paper is organized as follows. Section 2 describes the modeling of PEMFC, lithium-ion battery and UC, and clarifies the wavelet based load sharing and fuzzy logic based control algorithm developed for the hybrid system. Section 3 presents the simulation results of the hybrid vehicular system. Then, conclusions are given in Section 4.

2. System description and methodology

2.1. Modeling of a PEMFC

PEMFC in a hybrid vehicular system is the primary power source and should be operated for supplying the steady state load demand. The FC system model parameters utilized in the model development are as follows:

A	Activation area [cm^2 ($cell^{-1}$)]
B	Constant utilized in modeling of concentration overvoltage (V)
C	FC double-layer equivalent capacitance (F)
C_{O_2}	Dissolved oxygen concentration in the interface of the cathode catalyst
E_{Nernst}	Nernst instantaneous voltage (V)
F	Faraday constant [C $(kmol)^{-1}$]
I_{FC}	FC current (A)
J	Current density (A $(cm)^{-2}$)
J_{max}	Maximum current density [A $(cm)^{-2}$]
N_s	Number of series FCs in the stack
N_p	Number of FC stacks
P_{H_2}	Hydrogen partial pressure (atm)
P_{O_2}	Oxygen partial pressure (atm)
q_{H_2}	Amount of hydrogen flow required to meet the load change [kmol $(s)^{-1}$]
r_m	The resistivity of Nafion series proton exchanging membrane [Ω $(cm)^2$ m^{-1}]
R_a	Equivalent resistance representing the sum of the activation and concentration resistances (Ω)
R_c	The contact resistance between the membrane and electrodes (Ω)
R_m	Equivalent membrane impedance (Ω)
R_{ohmic}	FC internal ohmic resistance (Ω)
T	FC temperature (°K)
T_0, T_{rt}, T_{ic}, T_{it}	Empirical parameters utilized for modeling the variation of FC temperature
U	Utilization factor
V_{act}	Activation overvoltage (V)
V_d	Potential drop on R_a (V)
V_{conc}	Concentration overvoltage (V)
V_{ohmic}	Ohmic overvoltage (V)
V_{FC}	FC voltage (V)
V_{Stack}	Stack voltage (V)
λ	The water content of the membrane
ζ_1, ζ_2, ζ_3, ζ_4	Constants utilized in modeling of activation overvoltage

The ideal standard potential of a hydrogen/oxygen FC under standard state conditions (25 °C and 1 at.) is 1.229 V with liquid water product. However, the actual FC potential is lower than the ideal potential value due to the irreversible voltage drops occurring in FC systems. There are three types of irreversible voltage drops, namely activation overvoltage, ohmic overvoltage and concentration overvoltage. At low current densities, the activation overvoltage is responsible for the voltage drop of the FC. Besides, concentration overvoltage becomes more significant at high current densities. The effects of these voltage drops and the corresponding variance of FC voltage can be seen from the FC polarization curve in Fig. 1. The most efficient operating region for FC is the linear region corresponding to cell voltage between 0.55 V and

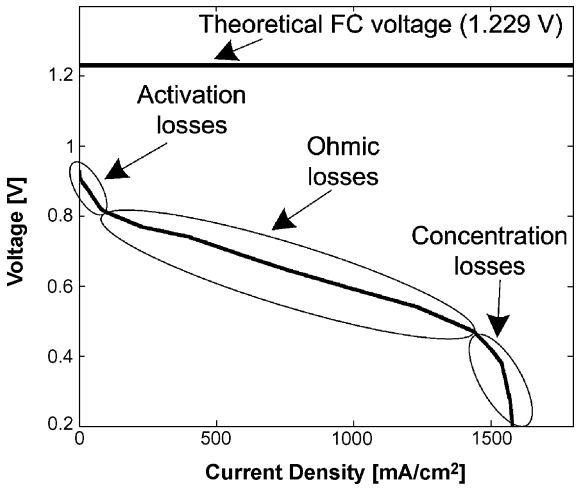

Fig. 1. Typical FC polarization curve.

0.8 V approximately, as seen from Fig. 1 [2,11]. Operating FC in this linear region is quite important for the overall system efficiency.

Considering the effects of the above mentioned irreversible voltage drops, the output voltage of FC can fundamentally be expresses as [12,13]

$$V_{FC} = E_{Nernst} - V_{act} - V_{conc} - V_{ohmic} \quad (1)$$

The Nernst's instantaneous voltage can be written as [14,15]

$$E_{Nernst} = 1.229 - (8.5 \times 10^{-4})(T - 298.15) + 4.308 \times 10^{-5} \times T \times \ln\left(P_{H_2} + \frac{1}{2}P_{O_2}\right). \quad (2)$$

Here, partial pressures of hydrogen and oxygen are considered to be changeable between predefined upper and lower limits for anode and cathode pressures inversely proportional to the molar flows of hydrogen and oxygen, and accordingly FC current. The molar flow of hydrogen that reacts in order to meet the load change can be found as

$$q_{H_2} = \frac{I_{FC} \times N_S \times N_P}{2FU} \quad (3)$$

Besides, the variation of the FC temperature expression in Eq. (2) can be calculated as [16]

$$T = 273 + T_0 + (T_0 - T_{rt} + T_{ic} \times I_{FC})\left(1 - \exp\left(-\frac{t \times I_{FC}}{T_{it}}\right)\right) \quad (4)$$

The following expression gives activation overvoltage occurring in FC system as [17,18]

$$V_{act} = \xi_1 + \xi_2 T + \xi_3 T(\ln(I_{FC})) + \xi_4(\ln(C_{O_2})) \quad (5)$$

In Eq. (5), the concentration of dissolved oxygen at the gas/liquid interface can be defined by a Henry's law expression of the form [17,19]

$$C_{O_2} = \frac{P_{O_2}}{5.08 \times 10^6 \exp(-498/T)} \quad (6)$$

Ohmic overvoltage in FC systems is the measure of the $I \times R$ voltage drop associated with the proton conductivity of the solid polymer electrolyte and electronic internal resistances. Thus, ohmic overvoltage in FC can be represented as [12]

$$V_{ohmic} = I_{FC} \times R_{ohmic} = I_{FC} \times (R_m + R_c). \quad (7)$$

The equivalent membrane impedance can be expressed in Ohm's law as

$$R_m = \frac{r_m \times \ell}{A}. \quad (8)$$

The resistivity of Nafion series proton exchange membrane in Eq. (8) can be calculated as [12,14]

$$r_m = \frac{181.6[1 + 0.03 \times J + 0.062 \times (T/303)^2 \times J^{2.5}]}{[\lambda - 0.634 - 3 \times J]\exp[4.18 \times (T - 303/T)]}. \quad (9)$$

where

$$J = \frac{I_{FC}}{A}. \quad (10)$$

Concentration overvoltage in FC systems is caused by the mass transportation which in turn affects the concentration of the hydrogen and oxygen at high current densities. The concentration overvoltage of FC can be expressed as [13]

$$V_{conc} = B \times \ln\left(1 - \frac{J}{J_{max}}\right). \quad (11)$$

One important electrochemical phenomenon linking the cell voltage to load current variations in FC systems is the charge double layer capacitor effect. The FC equivalent electrical circuit considering the charge double layer capacitor is shown in Fig. 2 [17]. This electrical capacitor represents the layer of charge on or near the electrode-electrolyte interface, which is a store of electrical charge and energy [18]. Considering the effects of this double layer capacitor effect, the dynamics of the FC output voltage can be obtained more accurately.

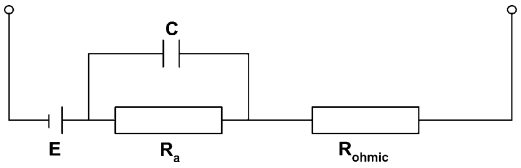

Fig. 2. FC electrical equivalent circuit [17].

The variation of the resistance R_a in Fig. 2, representing the sum of the activation resistance and concentration resistance, can be calculated as [18]

$$R_a = \frac{V_{act} + V_{conc}}{I_{FC}} \quad (12)$$

According to the aforementioned double layer capacitor effect, the differential equation related with the voltage drop on R_a can be written as [17,19]

$$\frac{dV_d}{dt} = \frac{I_{FC}}{C} - \frac{V_d}{R_a C} \quad (13)$$

Considering the combined effects of thermodynamics, mass transport, kinetics, and ohmic resistance, the variation of the FC output voltage can be calculated as follows [18,19]

$$V_{FC} = E_{Nernst} - V_d - V_{ohmic} \quad (14)$$

Finally, the voltage of an FC stack formed by N_s cells connected in series can be found as

$$V_{Stack} = N_s V_{FC}. \quad (15)$$

Fig. 3 shows the model of the PEMFC based on Eqs. (1)–(15), which is then embedded into the SimPowerSystems of MATLAB as a controlled voltage source and then integrated into the overall system.

2.2. Modeling of battery pack

In this study, a lithium-ion battery pack is utilized both for supplying a portion of the base load together with FC and capturing the braking energy together with UC. In this section, the dynamic model of the lithium-ion battery is introduced. The lithium-ion battery model parameters used in proposed model are as follows:

C_{bat}	Battery capacity (Ah)
I_{bat}	Battery current (A)
SOC_{bat}	Battery state of charge
$SOC_{bat.init}$	Initial battery state of charge
V_{bat}	Battery output voltage (V)
V_{OC}	Battery open-circuit voltage (V)
Z_{eq}	Battery equivalent internal impedance (Ω)

The battery output voltage can be calculated due to the battery open circuit voltage and voltage drop resulting from the battery equivalent internal impedance. Accordingly, the battery output voltage may be expressed as

$$V_{bat} = V_{OC} - i_{bat} Z_{eq} \quad (16)$$

The battery open circuit voltage is the difference of the electrical potential between the two terminals of a battery, when there is no external load connected. As the value of battery open circuit voltage

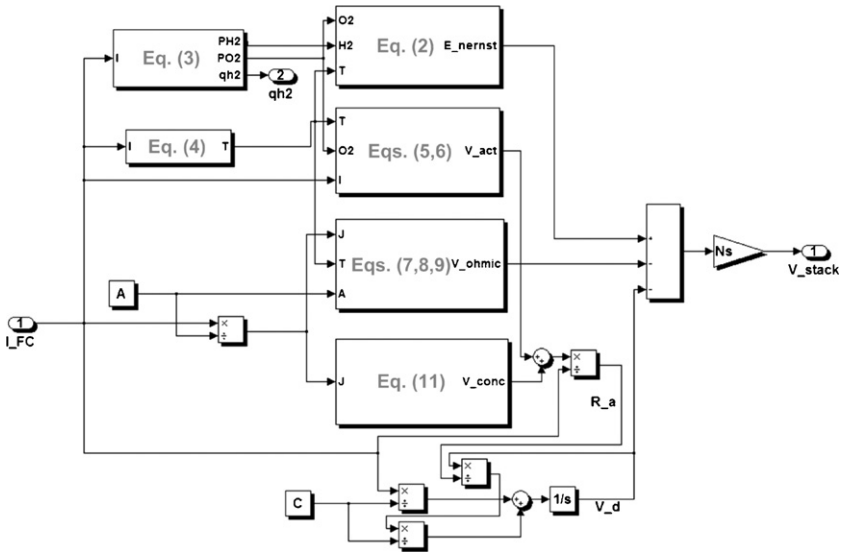

Fig. 3. Dynamic model of the FC system.

is strongly dependent on battery SOC, it can be calculated as [20]

$$V_{OC}(SOC_{bat}) = -1.031 \times \exp(-35 \times SOC_{bat}) + 3.685 + 0.2156 \times SOC_{bat} - 0.1178 \times SOC_{bat}^2 + 0.321 \times SOC_{bat}^3 \quad (17)$$

The battery SOC can be expressed as

$$SOC_{bat} = SOC_{bat\_init} - \int i_{bat}/C_{bat} dt. \quad (18)$$

The battery equivalent internal impedance in Eq. (16) consists of a series resistor (R_{series}), and two RC networks composed of $R_{Transient\_S}$, $C_{Transient\_S}$, $R_{Transient\_L}$ and $C_{Transient\_L}$, as shown in Fig. 4. R_{series} is responsible for the instantaneous voltage drop in battery terminal voltage. The components of RC networks are responsible for short and long-time transients in battery internal impedance. The values of R_{series}, $R_{Transient\_S}$, $C_{Transient\_S}$, $R_{Transient\_L}$ and $C_{Transient\_L}$ depending on battery SOC can be calculated due to the experimentally derived empirical equations given in Ref. [20].

The lithium-ion battery model used in the hybrid system is obtained by implementing the above mentioned equations in MATLAB&Simulink environment.

2.3. Modeling of UC bank

The natural structure of UC is appropriate to meet transient and instantaneous peak power demands. The UC bank is used to provide the difference between the load demand and the FC system

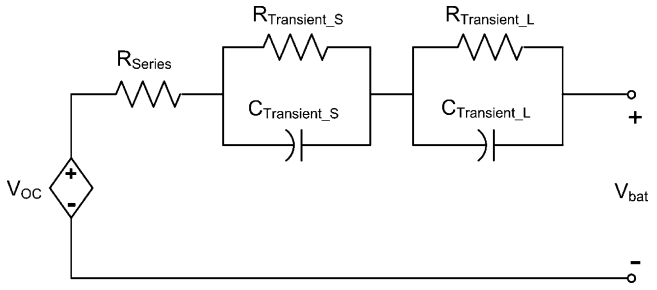

Fig. 4. Battery electrical equivalent circuit [20].

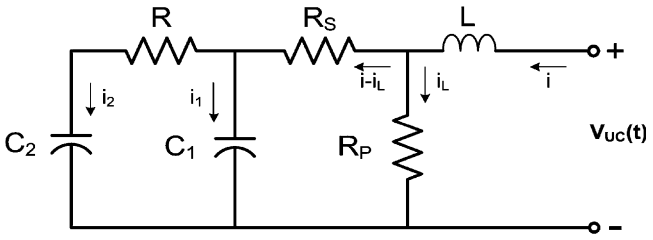

Fig. 5. UC electrical equivalent circuit.

output power. Fig. 5 shows the electrical equivalent circuit used in the UC model development. The developed model is verified by experimental studies using a Maxwell® 430 F, 16 V UC, which is currently operational in the authors' lab. Detailed description about the modeling of the UC system can be found in [21], which is a previous study of the authors.

2.4. Drive cycle

In order to evaluate the dynamic response of a developed methodology and make suggestions through the development in

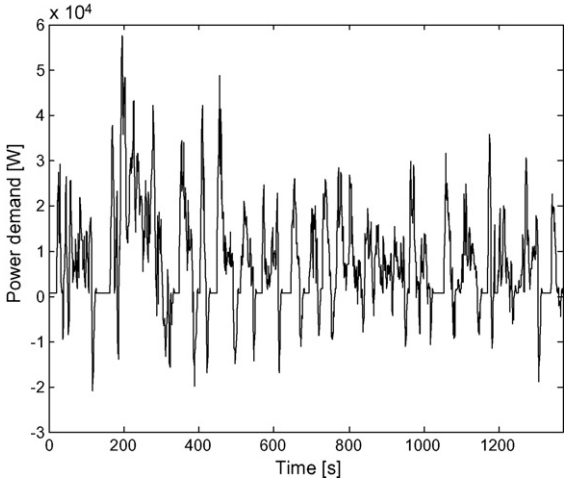

Fig. 6. Power demand of a vehicle according to UDDS cycle.

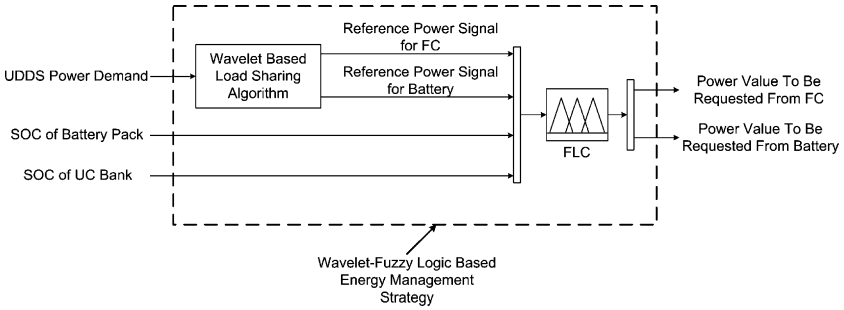

Fig. 7. A schematic diagram of the developed energy management strategy.

Table 1
Specific characteristics of UDDS cycle.

Time	1369(s)
Distance	7.45 (miles)
Max. speed	56.7 (mph)
Avg. speed	19.6 (mph)
Max. accel.	1.48 [m $(s^2)^{-1}$]
Max. decel.	−1.48 [m $(s^2)^{-1}$]
Avg. accel.	0.51 [m $(s^2)^{-1}$]
Avg. decel.	0.58 [m $(s^2)^{-1}$]
Idle time	259(s)

the overall structure, standard drive cycles can be utilized. To model the power demand of a vehicular system, UDDS cycle is used. UDDS cycle is a 1369-s test procedure designed to reflect typical speeds and accelerations in city traffic conditions in the United States. Fig. 6 shows the power demand in UDDS cycle as a function of time. Specific characteristics of the UDDS cycle are shown in Table 1.

2.5. Wavelet and fuzzy logic based energy management system

In this subsection, wavelet and fuzzy logic based energy management strategy developed for the hybrid vehicular system is introduced. A schematic diagram about the developed energy management system is shown in Fig. 7.

For better understanding of the power management strategies of hybrid vehicles with multiple on-board power sources, numerous studies realized by various authors can be found in the literature. Intelligent power management techniques are employed in Refs. [8,22,23]. Among them, fuzzy logic based control methodology has a major position due to its independence of a full mathematical plant model. Another power management method is realized in Ref. [24] for FC/battery hybrid structure. The mentioned model-based control in Ref. [24] targets the high fuel economy and system performance utilizing state observers. Many other power management techniques take place in the literature and a detailed literature survey on different power management techniques applied to hybrid vehicular systems can be found in Ref. [25]. The power manage-

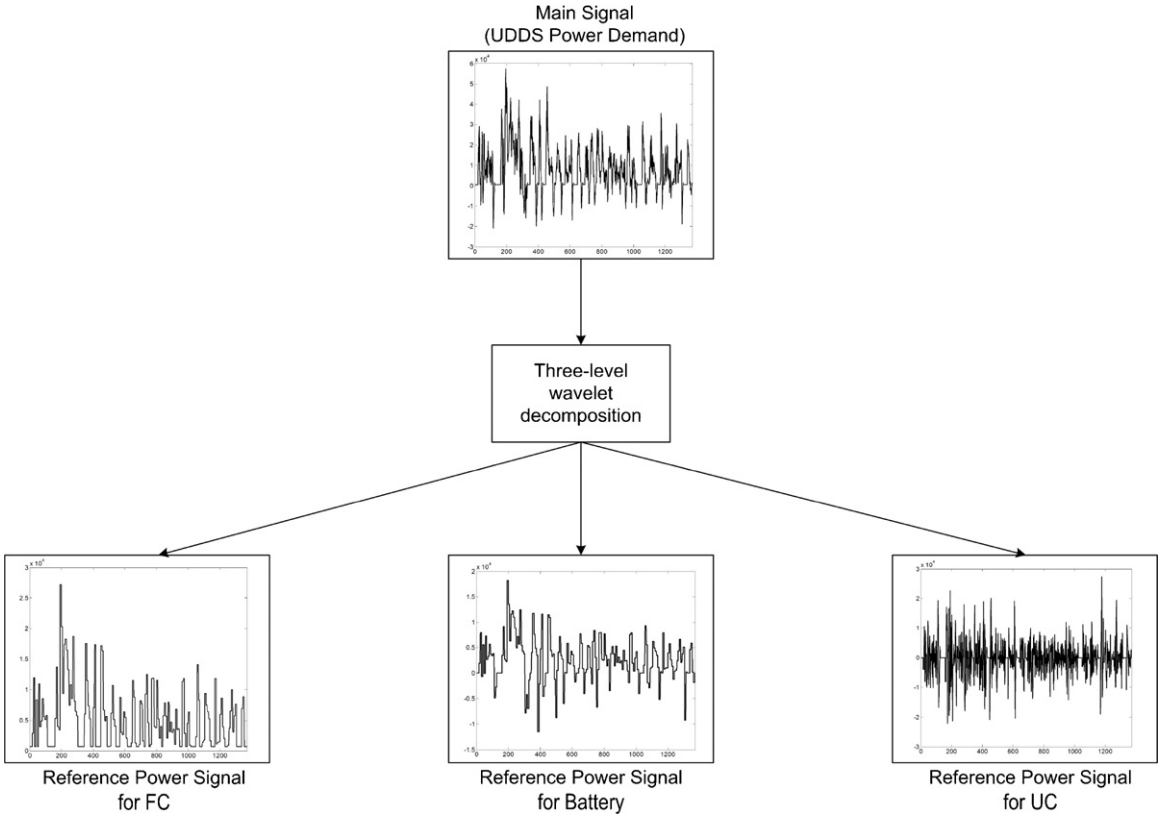

Fig. 8. Decomposition of the UDDS power profile using wavelet transform.

ment strategies mentioned above have proven their effectiveness in dealing with system efficiency. However, it cannot be guaranteed that the FC and battery systems can be protected from the power fluctuations in above studies. In order to overcome this issue, a wavelet-based energy management strategy is suggested in Refs. [9,10] for FC/UC and FC/Battery/UC hybrid vehicles. The transients in the total power demand profile are captured, a safe operating condition for FC-based electric vehicle can be provided and lifetime of the power sources can be extended. However, the fuel economy is not the main objective of the mentioned wavelet-based studies. The total energy efficiency can be promoted by decreasing the hydrogen consumption of FC. The combination of FLC and wavelet in this study ensures increment in both lifetime and fuel economy. Wavelet guarantees a stabilized output power for FC and battery, and FLC targets to achieve a better fuel economy as a master of the overall system power flow.

As mentioned before, the power demand of a vehicular system includes many sharp and instantaneous changes. Thus, the use of a load sharing algorithm that should isolate the base power demand of a vehicle from its transients is quite essential for the energy management of a hybrid system. For the development of a load sharing algorithm, we applied wavelet transform, since showing excellent performance in analyzing the transients in a given input signal.

Wavelet transform is a new mathematical approach that decomposes a time domain signal into different frequency groups and provides an effective manner for analyzing the non-stationary signals. In a wavelet transform, a fully scalable modulated time-window of varying size is applied for determining the locations of different frequencies. By employing the long windows at low frequencies and short windows at high frequencies, the wavelet transform is capable of comprehending the time and frequency information simultaneously [26]. Wavelet transform provides a quadrate mirror filtering application and the loss of important edge information is minimized compared to conventional filtering techniques [27]. The attractive features of wavelet transform in analyzing instantaneous variations make it possible to accurately capture and localize transient features in the data like the vehicle load profile [9,10]. Among different kinds of wavelets, Haar wavelet has the shortest filter length in the time domain. Besides, Haar wavelet is the simplest and most popular type of wavelet transform [9,10]. Hence in this study, we used a multi-level Haar wavelet transform as a load sharing algorithm. The main signal, UDDS power demand in this study, is decomposed into high frequency and low frequency components in three levels or subbands. UC is applied for satisfying the high frequency components. Then the low frequency component of the main signal is shared between FC and battery as battery supplies the negative parts and the positive parts of the low frequency signal up to 700 kW (base load in UDDS). Also FC and battery shares the positive parts above 700 kW, as FC supplies a portion of %60 while battery system supplies the rest %40 of the low frequency signal. The reference power signals for the hybrid system components obtained by the developed load sharing methodology are shown in Fig. 8. The detailed description about the mathematical basis of the proposed wavelet based load sharing algorithm can be found in Ref. [10].

Appropriate reference power signals for the characteristics of FC, battery and UC can be acquired by the proposed wavelet based load sharing algorithm. The smoothed FC and battery power signals are suitable for the FC and battery systems due to their slow response time to transients and negative effects of transients on their lifetimes. Besides, the rapid response capability of UC is convenient for delivering its reference power signal comprising of the transient components of UDDS load profile. However, an energy management strategy based only on a load sharing algorithm may not be sufficient enough for regulating all the system dynamics in desired range. The battery system and UC bank should have enough charge to supply the required load demand when the vehicle is accelerating and they should have enough capacity to recuperate energy during braking, which is rather important for increased fuel economy. Besides, the power to be requested from FC system should be decreased when both battery and UC have a normal SOC level. Hence, lower fuel consumption can be obtained. Thus, a control system which can supply a safe operating condition for FC and battery while controlling the overall system power flow with considering the SOC values of battery and UC should be applied in order to raise the effectiveness of the hybrid vehicular structure. As providing a control system, we used FLC, which provides a quite suitable manner for the control of hybrid energy systems [28].

According to many researchers, there are some reasons for the present popularity of FLC over conventional control methods. Nonlinearity and difficulties in proper identification of parameters of the plant mathematical models limit the use of model based conventional control approaches. FLC utilizes more information from experts and does not require an overall mathematical model about a physical system as compared to conventional methods. Thus, FLC provides a pretty suitable structure especially for the systems composed of nonlinear behaviors where an overall mathematical model is difficult to obtain [29]. Thanks to the above mentioned useful features of FLC, it has a suitable structure for the control of vehicular applications.

The FLC utilized in this study has 4 inputs and 2 outputs as shown in Fig. 7. The inputs of the FLC are the reference power signal of FC and the reference power signal for battery that are generated by the wavelet based load sharing algorithm, and the SOC values of the battery pack and UC bank. Using the data available from these four inputs, the FLC determines the power value to be requested from FC and battery. The rule base of the developed FLC is clarified in Fig. 9. The rule base of the developed FLC consists of two parts: the power distribution when the vehicle is accelerating and decelerating/braking. The main target of the applied control methodology is decreasing the fuel consumption by using battery and/or UC instead of FC system as much as possible whenever they have enough charge. Firstly, considering the accelerating periods of vehicle, the rule base is generated as seen from Fig. 9. Besides, distribution of available braking energy between battery and UC in deceleration periods of the vehicle performs the second part of FLC rule base. In deceleration periods, FLC follows the variations of battery and UC SOC values, and then shares the braking energy between battery and UC. In normal conditions of both SOC values, battery absorbs the reference braking energy. However, if the SOC value of UC is lower than expected, then the battery captures less braking energy and the rest of the battery reference braking energy is recycled by UC. Besides, if SOC of UC is more than desired or SOC of battery is in a low region, then FLC determines a requested battery power more than the reference battery power of braking condition in order to discharge UC or charge battery. Thus, SOC of both battery and UC can be controlled within a suitable range while FC and battery transfer power in an appropriate manner without subjecting to transients, which is provided by the wavelet transform based load sharing algorithm. In short, the operating lifetimes of FC and battery may significantly be increased while the fuel economy and system performance should be promoted by the applied energy management strategy.

2.6. Power conditioning unit

The power conditioning unit applied to the developed hybrid system is clarified in this subsection. For the parallel operation of different power sources, various topologies may be utilized [8,9,30]. In this study, we provide a power conditioning unit using three dc/dc converters employed for power tracking and voltage regulation, as shown in Fig. 10. The proper response of the hybrid system to

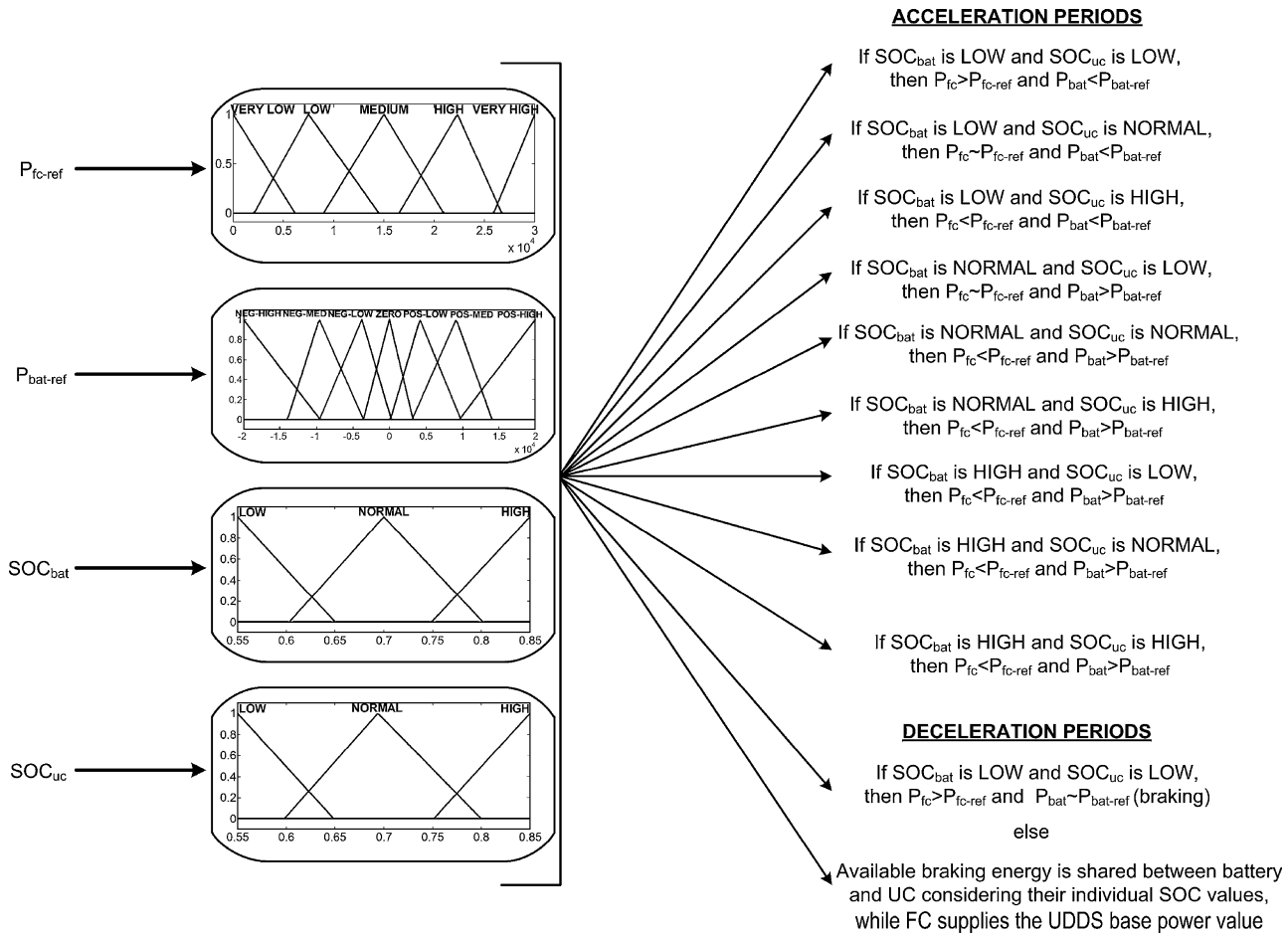

Fig. 9. Fuzzy logic controller rule base.

the overall load dynamics can be achieved by generating appropriate switching signals to the dc/dc converters. A similar methodology for the control of DC/DC converters can be found in Ref. [31]. This kind of control for three dc/dc converters is also advised in Ref. [9], as the dc/dc converter of one of the available power sources is employed for the dc bus voltage regulation which is called "voltage-oriented-control", and the rest of the converters are controlled for power tracking by "power-oriented-control" methodology.

In this study, the boost type dc/dc converter of the FC system and the bidirectional type dc/dc converter of the battery pack are used to supply the power value determined by fuzzy logic control system from both sources. Besides the bidirectional type dc/dc converter of the UC bank is employed for regulating the load bus voltage. As the power density of UC is much higher than that of battery, UC is utilized for the voltage regulation. For the realized voltage control, the measured dc bus voltage is compared to the reference voltage value, 188 V in this study, and then the error signal is processed in a PI controller. In the acceleration periods, PI controller generates appropriate duty cycles in order to increase the bus voltage to its reference. Besides, during the braking periods, the dc bus voltage increases and the PI controller regulates the bus voltage and provides the capability of transferring the available braking energy to UC. The similar control logic is applied for battery system power tracking process. The output power value of the battery pack is compared with the requested battery power obtained by the FLC. Then, by processing the error signal in a PI controller, a bidirectional power transfer can be achieved. Thus, battery transfers the requested power value to the load and the braking energy can be recycled. Furthermore, the unidirectional power flow of FC can again be controlled by a PI controller employed for the boost dc/dc converter of FC. The transfer of the requested power from FC to the power train can be realized by the FC system power tracking process. Thus, the proposed power conditioning unit provides the capability of delivering the desired power value from the hybrid power sources while keeping the bus voltage in a desired level.

3. Test and results

In the simulation process, the aim is to observe and evaluate the proposed hybrid system behavior and performance during a drive cycle obtained by real life drive conditions. Simulation results for the proposed FC/Battery/UC hybrid vehicular system shown in Fig. 10 are obtained using MATLAB, Simulink and SimPowerSystems based software packages by implementing the mathematical and electrical models of the system.

Different designs of PEMFC, battery and UC bank can be performed for different applications. The sizing of the hybrid system components is realized considering the reference power signals for FC, battery and UC shown in Fig. 8. And the technical specifications of 50 kW NedStack PS50 PEMFC, Panasonic NCR18650E lithium-ion battery and Maxwell Boostcap® BMOD0430 UC are considered for the sizing methodology. The PEMFC system parameters used in this study are shown in Table 2. The rated output power of PS50 per cell is 80 W [32]. Thus, the rated output power of the FC module consisting of 176 × 2 = 352 cells is 28.2 kW. Thus, the reference power signal for FC shown in Fig. 8 can completely be satisfied. Besides, the battery characteristics for a cell are shown in Table 3, which are derived by Panasonic CGR18650E lithium-ion battery [33]. For the devel-

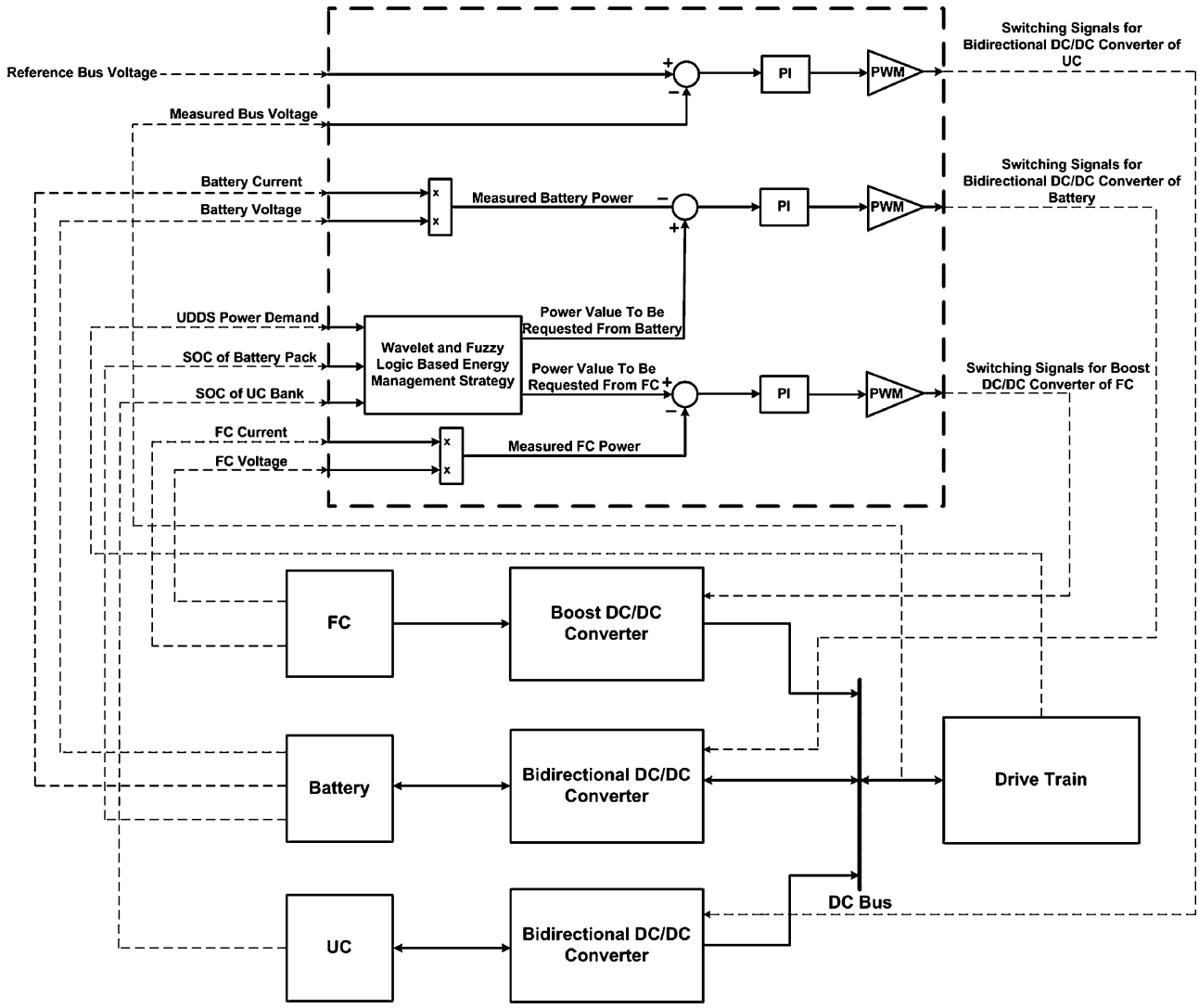

Fig. 10. Hybrid system configuration.

oped hybrid system, we composed a battery pack with 40 parallel connected strings. Each string consists of 45 battery cells connected in series. The nominal voltage of this battery is 3.6 V. Additionally the nominal capacity of PANASONIC NCR18650E lithium-ion battery cell is 2.9 Ah. So the nominal power of the battery pack is 18.8 kW. The analysis shows that this simulated battery pack can completely meet the requirements delineated in Fig. 8. Moreover for this study, we selected the Maxwell Boostcap® BMOD0430 UC unit, whose characteristics are shown in Table 4 [34]. Each UC unit has a

Table 2
FC system model parameters.

Activation area (A)	6.25 [cm^2 (cell^{-1})]
Constant utilized in modeling of concentration overvoltage (B)	0.016 (V)
FC double-layer equivalent capacitance (C)	2.5 (F)
Faraday constant (F)	96486.7 [C (kmol)$^{-1}$]
Maximum current density (J_{max})	1.5 [A (cm)^2]
Number of series FCs in the stack (N_s)	176
Number of FC modules (N_p)	2
The contact resistance between the membrane and electrodes (R_c)	2×10^{-4} (Ω)
Empirical parameters utilized for modeling the variation of FC temperature (T_0,T_{rt},T_{ic},T_{it})	28, 20, 0.7, 4000
Utilization factor (U)	0.8
Constants utilized in modeling of activation overvoltage (ζ_1,ζ_2,ζ_3,ζ_4)	−0.9514, 0.00312, 7.4×10^{-5}, -1.87×10^{-4}

Table 3
Panasonic NCR18650E lithium-ion battery cell specifications [32].

Nominal Voltage	3.6 (V)
Standard Capacity	2900 (mAh)
Diameter	18.6 (mm)
Height	65.2 (mm)
Weight	45 (g)

Table 4
Maxwell Boostcap BMOD0430 P016 ultra-capacitor specifications [33].

Capacitance	430 (F)
Voltage	16.2 (V)
Dc resistance	2.5 (mΩ)
Ac resistance (@ 1 kHz)	2.0 (mΩ)
Weight	5.5 (kg)
Volume	4.7 (L)

Table 5
Weight and volume comparison of the developed FC/Battery/UC hybrid system with FC/UC hybrid structure.

		FC/UC hybrid [21]	FC/Battery/UC hybrid
FC	Weight (kg)	352	232.3
	Volume (m^3)	0.394	0.2604
Battery	Weight (kg)	–	81
	Volume (m^3)	–	0.1275
UC	Weight (kg)	66	55
	Volume (m^3)	0.0564	0.047
Total	Weight (kg)	418	368.3
	Volume (m^3)	0.4504	0.4349

nominal voltage of 16 V with a capacitance of 430 F. Since we have an experimentally validated simulation model for Maxwell Boostcap® BMOD0430 UC, this module is selected in this study. The UC bank consists of 2 parallel connected strings. Each string includes 5 UC units connected in series. The UC bank must be capable of supplying the maximum power value of the UC reference power signal (28 kW) in Fig. 8 for 10 s. Thus, the proposed UC bank design must have a minimum rating of $(28000/0.75) \times (10/3600) = 103.7$ Wh. The proposed UC unit has a capacitance of $430 \times (2/5) = 172$ F and a voltage of $16 \times 2 = 80$ V, corresponding to 152.88 Wh of energy. Thus, this UC bank design can easily meet the required amount of energy. To conclude, it can be seen that the overall hybrid system design can satisfy the requirements of UDDS cycle as well as the developed energy management strategy.

In order to compare the weight and volume of the developed FC/Battery/UC hybrid system with FC/UC hybrid structure, again the technical specifications of 50 kW NedStack PS50 PEMFC, Panasonic NCR18650E lithium-ion battery and Maxwell Boostcap® BMOD0430 UC are considered. The weight and volume values for NedStack PS50 per cell are 0.66 kg and 0.00074 m^3, approximately [32]. Moreover, NCR18650E lithium-ion battery has a 0.0000708 m^3 volume and a 0.045 kg weight per cell [33]. Lastly, each BMOD0430 UC unit has a volume of 4.7 L (corresponding to 0.0047 m^3) with a weight of 5.5 kg [34]. In the previous study of the authors [21], the total volume and weight of a FC/UC hybrid system are approximately calculated as 418 kg and 0.4504 m^3, respectively, as shown in Table 5. In the mentioned study, the utilized PEMFC was composed of $176 \times 3 = 528$ cells while UC bank was constructed with $6 \times 2 = 12$ UC modules. For comparison, the PEMFC system utilized in this study consisting of 352 cells has a weight of 2323 kg and a volume of 0.26 m^3. In addition, the volume and weight of the overall UC bank consisting of $5 \times 2 = 10$ UC units are 47 L (corresponding to 0.047 m^3) and 55 kg, respectively. Furthermore, the battery system composed of $45 \times 40 = 1800$ cells covers a volume of 0.1275 m^3 and weights 81 kg, approximately. Thus, the overall PEMFC/Battery/UC hybrid system has a total volume of 0.4349 m^3 and a weight of 368.3 kg. As clearly seen from the above calculations, the FC/Battery/UC hybrid system provides a lightweight structure with almost the same volume as compared to FC/UC hybrid structure.

To illustrate the performance of the developed methodology, FC system output power, battery pack power, UC bank power, FC stack voltage, SOC of battery pack, SOC of UC bank, dc load voltage and amount of hydrogen flow required under load changes as a function of time are given in Figs. 11–19, respectively.

The variation of FC output power is demonstrated in Fig. 11. It is obvious from Fig. 11 that the FC system satisfies a base portion of the load power without facing to transient changes. Thus, it is supposed to acquire a crucial increase in FC lifetime by the proposed energy management strategy. The maximum power generated by the FC system is 26005 W, when the load demand is at the highest level. A sole FC system employed for the propulsion of such a vehi-

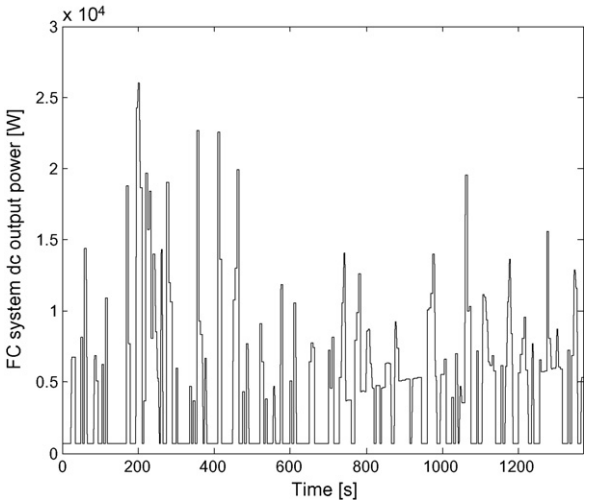

Fig. 11. The variation of FC system dc output power.

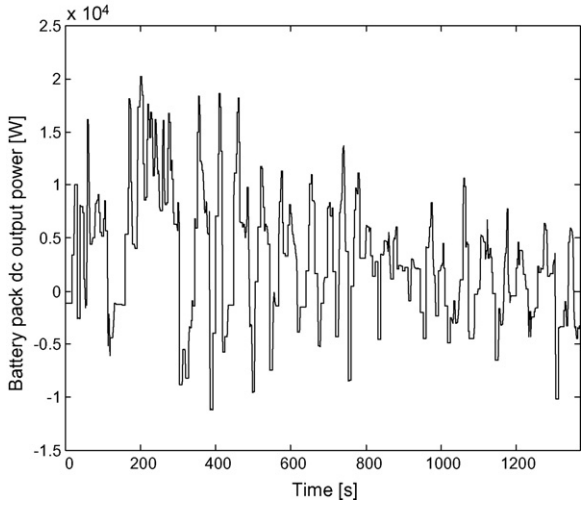

Fig. 12. The variation of battery pack charging and discharging power.

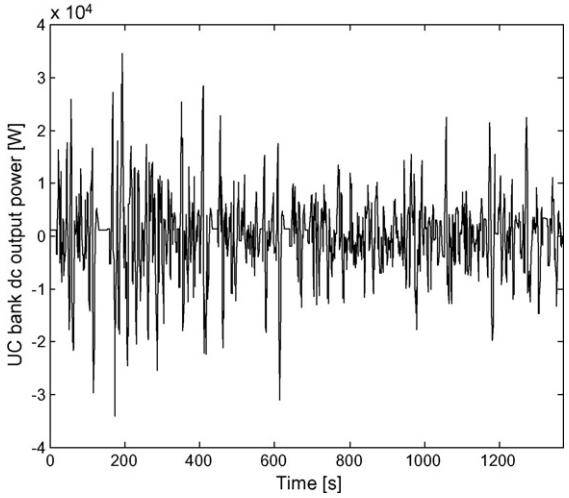

Fig. 13. The variation of UC bank charging and discharging power.

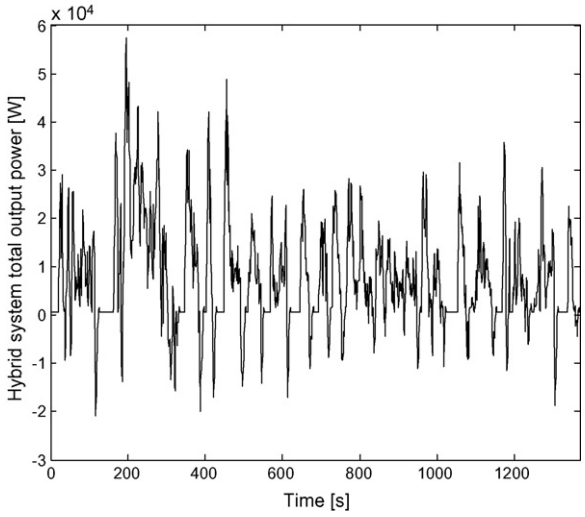

Fig. 14. Total output power of the hybrid system.

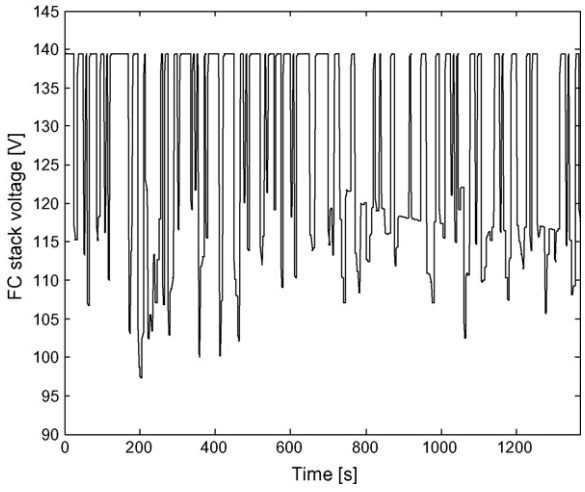

Fig. 15. The variation of FC stack voltage.

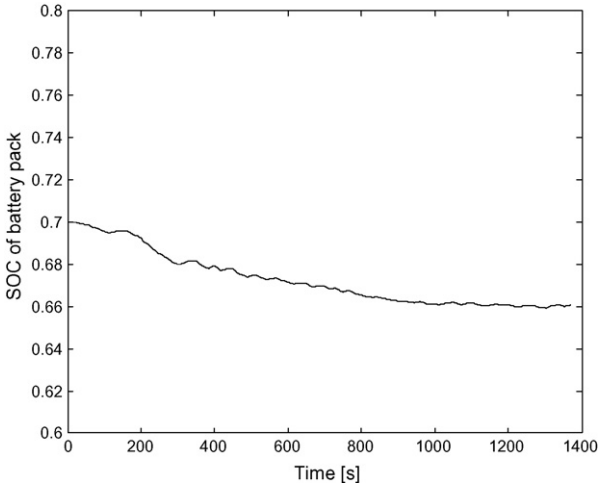

Fig. 16. The variation of state-of-charge of the battery pack.

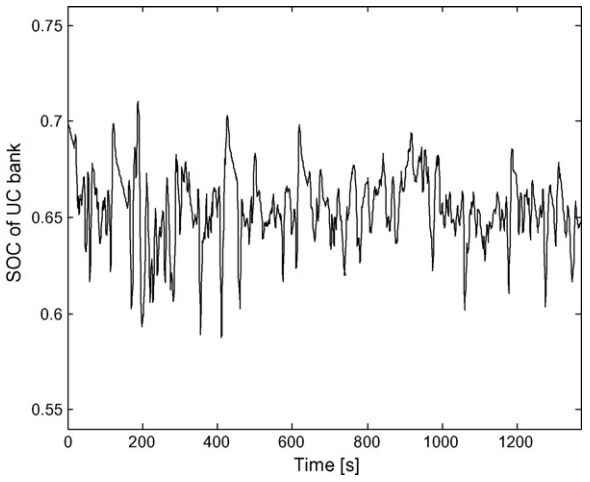

Fig. 17. The variation of state-of-charge of the UC bank.

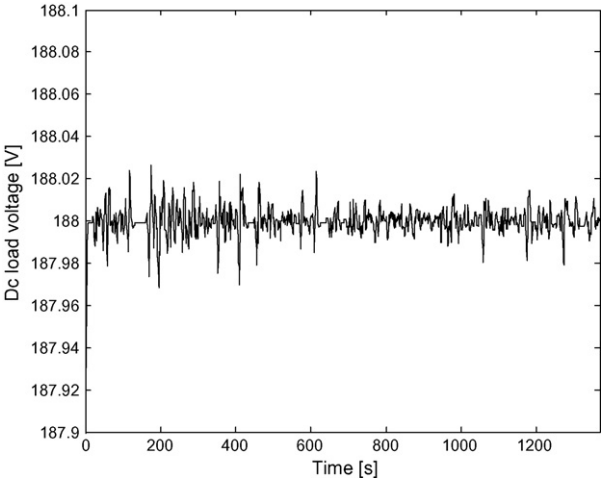

Fig. 18. The variation of dc load voltage.

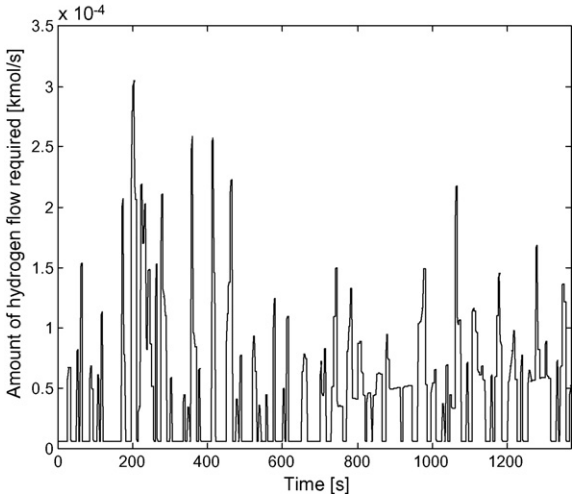

Fig. 19. The variation of the amount of hydrogen flow required to meet the load change.

cle would have to supply a higher power value while confronting sharp peak loads. The hybridization of FC with both battery and UC provides the merit of decreasing the size and cost of FC system as compared a sole FC system or FC/UC hybrid structure as mentioned before.

The charge and discharge power of the battery pack is illustrated in Fig. 12. The positive and negative power regions of Fig. 12 represent the transmitted power to the drive train and the captured power by the battery pack, respectively. It can clearly be seen in Fig. 12 that the battery pack helps FC to supply the steady state load demand and attends to the low frequency part of the braking energy as supposed in the development of the energy management strategy. Thus, the electrochemical structure of battery is not disturbed by sudden load variations and a safe operation for battery can be obtained, which accordingly promotes the battery operational lifetime. Besides, the UC bank output power alternates between negative and positive according to charging or discharging, as depicted in Fig. 13. UC bank successfully supplies all the power demand fluctuations and provides a great response capability to all load changes for the developed hybrid system. Besides, the hybrid system total output power which is the sum of the individual FC, battery and UC powers is shown in Fig. 14. It is evident from Fig. 14 that the hybrid system successfully satisfies the load demand shown in Fig. 8.

It is clear from Fig. 15 that an increase in the load decreases the output voltage of the FC stack. Under different conditions of UDDS cycle, FC stack voltage varies in a suitable range, from 97.1 V to 139.4 V, corresponding to a voltage interval between 0.56 V and 0.79 V per cell, as seen from Fig. 15. It is evident that FC system is operated in linear region during the entire UDDS cycle. Thus, the efficiency of FC system is increased, which accordingly promotes the overall system efficiency. If a sole FC system were applied for the vehicle propulsion, the mentioned voltage variation interval would be significantly larger causing lower system efficiency, thus showing the importance of FC combination with ESS on efficient operation.

Figs. 16 and 17 show the SOC variations of battery and UC with respect to the load changes, respectively. From Figs. 16 and 17, it is clear that the proposed control algorithm can successfully maintain the SOC values of battery and UC within suitable limits. The SOC of battery changes between 0.659 and 0.7 while SOC of UC fluctuates between 0.588 and 0.711. FLC ensures that battery and UC always have enough charge for the accelerating periods while regulating the system power flow with the aim of decreasing fuel consumption. Thus, both battery and UC bank can effectively supply the required load demand and fuel economy can be promoted.

The variation of dc load voltage due to load changes is demonstrated in Fig. 18. The load voltage varies in a suitable interval as shown in Fig. 18, which indicates that the load bus voltage is kept within acceptable limits by generating proper duty signals for the UC bidirectional converter. Besides, the amount of hydrogen flow required to respond the load changes varies as illustrated in Fig. 19. The downsizing of FC system provides a significant hydrogen economy as compared to a FC only or a FC/UC hybrid system, thus clarifies the advantage of the proposed methodology. Moreover, in order to exhibit the importance of FLC based control methodology, the fuel consumption comparison is realized between the proposed wavelet-FLC based energy management strategy and only wavelet-based energy management strategy without using FLC. The overall fuel consumption with the proposed energy management methodology is calculated as 0.06421 kmol H_2 during the UDDS cycle. Besides, only wavelet-based energy management strategy without FLC provides a fuel consumption of 0.06962 kmol H_2. Thus, using FLC promotes the fuel economy (∼%8) as supposed in the energy management system development.

4. Conclusions

This paper introduces an energy management strategy based on wavelet transform and fuzzy logic to control power distribution in a hybrid PEMFC/Battery/UC vehicular system. The FC and battery together satisfy the base load while battery and UC jointly absorb the regenerative braking energy of the vehicular system. An experimentally verified UC model is utilized in the proposed hybrid structure.

As compared to a FC/UC hybrid structure, the proposed FC/Battery/UC hybrid system has a lightweight structure. Simulation results of the developed methodology for the FC/Battery/UC hybrid vehicular system are encouraging and indicate viability of the proposed energy management technique. The power references acquired by wavelet transform for the FC and battery have a limited slope to avoid fast load variations in these power sources. Besides, UC system supplies the extra transient demands owing to its great fast response capability. Thus, it is expected to achieve a good performance, efficiency, and durability of individual power sources. Moreover, the SOC value of both battery and UC can be maintained within suitable limits, which accordingly results in a considerable increase in fuel economy. Furthermore, the FC system can be operated in its most efficient linear region. Last but not least, the decrease in the size of FC system lowers the system cost as well as the fuel consumption. Consequently, the combination of FLC and wavelet can offer increment in both lifetime and fuel economy as wavelet guarantees a transient-free output power for FC and battery, and FLC provides a better fuel economy as the master of the overall system power flow.

Acknowledgement

This work was supported in part by the Scientific and Technological Research Council of Turkey (TUBITAK) under Grant 107M355.

References

[1] R.K. Ahluwalia, X. Wang, Fuel cell systems for transportation: status and trends, J. Power Sources 177 (1) (2008) 167–176.
[2] F. Barbir, PEM Fuel Cells: Theory and Practice, Elsevier Academic Press, London, UK, 2005.
[3] Z. Liu, L. Yang, Z. Maoa, W. Zhuge, Y. Zhang, L. Wang, Behavior of PEMFC in starvation, J. Power Sources 157 (1) (2006) 166–176.
[4] M. Kim, Y.J. Sohn, W.Y. Lee, C.S. Kim, Fuzzy control based engine sizing optimization for a fuel cell/battery hybrid mini-bus, J. Power Sources 178 (2) (2008) 706–710.
[5] B. Kennedy, D. Patterson, S. Camilleri, Use of lithium-ion batteries in electric vehicles, J. Power Sources 90 (2) (2000) 156–162.
[6] V. Paladini, T. Donateo, A.D. Risi, D. Laforgia, Super-capacitors fuel-cell hybrid electric vehicle optimization and control strategy development, Energy Conversion Manage. 48 (11) (2007) 3001–3008.
[7] A.D. Pasquier, I. Plitz, S. Menocal, G. Amatucci, A comparative study of Li-ion battery, supercapacitor and nonaqueous asymmetric hybrid devices for automotive applications, J. Power Sources 115 (1) (2003) 171–178.
[8] D. Gao, Z. Jin, Q. Lu, Energy management strategy based on fuzzy logic for a fuel cell hybrid bus, J. Power Sources 185 (1) (2008) 311–317.
[9] X. Zhang, C.C. Mi, A. Masrur, D. Daniszewski, Wavelet-transform-based power management of hybrid vehicles with multiple on board energy sources including fuel cell, battery and ultracapacitor, J. Power Sources 185 (2) (2008) 1533–1543.
[10] M. Uzunoglu, M.S. Alam, Modeling and analysis of an FC/UC hybrid vehicular power system using a novel wavelet based load sharing algorithm, IEEE Trans Energy Conversion 23 (1) (2008) 263–272.
[11] M.C. Kisacikoglu, M. Uzunoglu, M.S. Alam, Load sharing using fuzzy logic control in a fuel cell/ultra-capacitor hybrid vehicle, Int. J. Hydrogen Energy 34 (3) (2009) 1497–1507.
[12] J.M. Andujar, F. Segura, M.J. Vasallo, A suitable model plant for control of the set fuel cell-DC/DC converter, Renewable Energy 33 (4) (2008) 813–826.
[13] S.K. Park, S.Y. Choe, Dynamic modeling and analysis of a 20-cell PEM fuel cell stack considering temperature and two-phase effects, J. Power Sources 179 (2) (2008) 660–672.
[14] R.F. Mann, J.C. Amphlett, M.A.I. Hooper, H.M. Jensen, B.A. Peppley, P.R. Roberge, Development and application of generalized steady-state electrochemical model for a PEM fuel cell, J. Power Sources 86 (1–2) (2000) 173–180.

[15] X. Xue, J. Tang, A. Smirnova, R. England, N. Sammes, System level lumped parameter dynamic modeling of PEM fuel cell, J. Power Sources 133 (2) (2004) 188–204.
[16] Z. Zhang, X. Huang, J. Jiang, B. Wu, An improved dynamic model considering effects of temperature and equivalent internal resistance for PEM fuel cell power models, J. Power Sources 161 (2) (2006) 1062–1068.
[17] P.R. Pathapati, X. Xue, J. Tang, A new dynamic model for predicting transient phenomena in a PEM fuel cell system, Renewable Energy 30 (1) (2005) 1–22.
[18] K.P. Adzakpa, K. Agbossou, Y. Dube, M. Dostie, M. Fournier, A. Poulin, PEM fuel cells modeling and analysis through current and voltage transient behaviors, IEEE Trans Energy Conversion 23 (2) (2008) 581–591.
[19] M.J. Khan, M.T. Iqbal, Dynamic modeling and simulation of a small wind–fuel cell hybrid energy system, Renewable Energy 30 (3) (2005) 421–439.
[20] M. Chen, G.A.R. Mora, Accurate electrical battery model capable of predicting runtime and I-V performance, IEEE Trans Energy Conversion 21 (2) (2006) 504–511.
[21] O. Erdinc, B. Vural, M. Uzunoglu, Y. Ates, Modeling and analysis of an FC/UC hybrid vehicular power system using a wavelet-fuzzy logic based load sharing and control algorithm, Int. J. Hydrogen Energy, in press, doi:10.1016/j.ijhydene.2008.10.039.
[22] D.V. Prokhorov, Toyota Prius HEV neurocontrol and diagnotics, Neural Networks 21(2–3) (458) 458–465.
[23] C.Y. Li, G.P. Liu, Optimal fuzzy power control and management of fuel cell/battery hybrid vehicles, J. Power Sources, in press, doi:10.1016/j.jpowsour.2009.03.007.
[24] Y. Haitao, Z. Yulan, S. Zechang, W. Gang, Model-based power control strategy development of a fuel cell hybrid vehicle, J. Power Sources 180 (2) (2008) 821–829.
[25] F.R. Salmasi, Control strategies for hybrid electric vehicles: evolution, classification, comparison and future trends, IEEE Trans Vehicular Technology 56 (5) (2007) 2393–2404.
[26] S.P. Valsan, K.S. Swarup, Wavelet based transformer protection using high frequency power directional signals, Electric Power Syst. Res. 78 (4) (2008) 547–558.
[27] S. Osowski, K. Garanty, Forecasting of the daily meteorological pollution using wavelets and support vector machine, Eng. Appl. Artificial Intelligence 20 (6) (2007) 745–755.
[28] C.T. Leondes, Fuzzy Logic and Expert Systems Application, Academic Press, California, USA, 1998.
[29] I. Eker, Y. Torun, Fuzzy logic control to be conventional method, Energy Conversion Manage. 47 (4) (2006) 377–394.
[30] Honda Fuel Cell Power FCX. Available: http://world.honda.com/FuelCell/FCX/FCXPK.pdf, December 2004, press information (online).
[31] A.A. Ferreira, J.A. Pomilio, G. Spiazzi, L.A. Silva, Energy management fuzzy logic supervisory for electric vehicle power supplies system, IEEE Trans Power Electronics 23 (1) (2008) 107–115.
[32] NedStack PS50 Product Data. Available: http://www.nedstack.com/docs/ps50.pdf, (Online).
[33] Panasonic NCR18650E lithium-ion battery product data. Available: http://www.panasonic.ca/English/batteries/industrialbatteries/lithiumionspecs.asp, (Online).
[34] Electric Double Layer Capacitor: Boostcap® Ultracapacitor. Available: http://www.maxwell.com/pdf/uc/datasheets/eol/mc power series1009363 rev2.pdf, (Online).